ISSN 1063-7850, Technical Physics Letters, 2015, Vol. 41, No. 3, pp. 284–287. © Pleiades Publishing, Ltd., 2015.
Original Russian Text © I.V. Kireeva, Yu.I. Chumlyakov, Yu.N. Platonova , 2015, published in Pis'ma v Zhurnal Tekhnicheskoi Fiziki, 2015, Vol. 41, No. 6, pp. 58–66.

The Effect of Hydrogen on Shape Memory Effect and Superelasticity in Single-Phase Nickel Titanium Single Crystals

I. V. Kireeva*, Yu. I. Chumlyakov, and Yu. N. Platonova
Siberian Physicotechnical Institute, Tomsk State University, Tomsk, 634050 Russia
**e-mail: kireeva@spti.tsu.ru*

Received October 3, 2014

Abstract—The effect of hydrogen on temperature dependences of axial stresses $\sigma_{cr}(T)$, shape memory effect, and superelasticity of $[\bar{1}11]$-oriented Ti–50.7% Ni (at %) alloy single crystals has been studied under tensile strain in a single-phase state. It is established that the level of $\sigma_{cr}(M_s)$ and σ_{cr}(B2) stresses is determined by the state of hydrogen (in solid solution or titanium hydride particles) in the initial B2 phase. Superelasticity up to 2.0–2.5% occurs when hydrogen is present in the solid solution.

DOI: 10.1134/S1063785015030232

Nickel titanium (TiNi) alloys are widely used in technology and medicine due to their unique functional properties—shape memory effect (SME) and superelasticity (SE) [1, 2]. As is known [2], both components (nickel and titanium) of TiNi alloys are hydride-forming metals. Investigations of the effect of hydrogen on the martensite transformations (MTs) in TiNi polycrystals [2–5] have shown that the presence of hydrogen changes start temperature M_s of the forward MT on cooling, decreases stability of the crystalline lattice of the B2 phase, reduces plasticity at high hydrogen concentrations, and favors the formation of oriented martensite during hydrogenation [3, 4].

The present work was aimed at determining the influence of hydrogen on temperature dependences of critical axial stresses $\sigma_{cr}(T)$ in a temperature interval of T = 173–473 K and on the SME and SE effects in $[\bar{1}11]$-oriented Ti–50.7% Ni (at %) alloy single crystals under tensile strain in a single-phase state. The study on single crystals allow to exclude inhomogeneity of hydrogen distribution between the volume and boundaries of grain. The $[\bar{1}11]$ orientation of single crystals for studying the effect of hydrogenation was selected due to its maximum recoverable strain (ε_0 = 9.8%) in tension for B2–B19' MT [6].

Single crystals of Ti–50.7% Ni (at %) alloy were grown in a helium atmosphere using the Bridgman technique. The as-grown samples were homogenized at T = 1173 K for 12 h in an inert gas atmosphere, followed by quenching in water. The orientation of crystals and their phase composition were determined by X-ray diffraction on a DRON-3 instrument using FeK_α radiation. The samples for tensile testing were shaped as standard double pads with 12 × 2.5 × 1-mm working part dimensions. The samples were electrochemically hydrogenated in aqueous 4% H_2SO_4 solution at T = 295 K and current density j = 1400 A/m^2 for a period of time within 2–4 h in a cell with an austenite stainless steel anode. The mechanical tensile tests were carried out on an Instron 5969 machine at a straining rate of 4×10^{-4} s^{-1} at temperatures from 173 to 473 K. The characteristic MT temperatures were determined by the well-known method using characteristic bending points on temperature dependences of electric resistivity $\rho(T)$.

Single-phase single crystals of Ti–50.7% Ni (at %) alloy exhibit a single-stage B2–B19' MT with the fol-

Mechanical and functional characteristics of B2–B19' MT in $[\bar{1}11]$ single crystals of Ti–50.7% Ni (at %) alloy before and after hydrogenation

Characteristics of B2–B19' MT	Without H_2	2 h H_2	4 h H_2
M_s, K at σ = 0 MPa	175	200	223
MT temperatures at σ = 75 MPa:			
M_s^σ, K	214	207	231
M_f^σ, K	178	117	145
A_s^σ, K	235	216	243
A_f^σ, K	272	268	275
Δ_1/Δ_2 under σ, K	36/37	90/52	86/32
Γ_1/Γ_2, K	58/57	61/99	44/98
$\sigma_{cr}(M_s)/\sigma_{cr}$(400 K), MPa	25/530	40/650	80/560
$\alpha = d\sigma_{cr}/dT$, MPa/K	4.26	4.6	4.6

lowing start and finish temperatures for the forward (cooling) and reverse (heating) transitions: $M_s = 175$ K, $M_f = 133$ K, $A_s = 192$ K, and $A_f = 233$ K. Figure 1 shows the temperature dependences of axial stresses σ_{cr} in tensile-strained TiNi single crystals measured before and after hydrogenation. As can be seen, $\sigma_{cr}(T)$ curves in both cases reveal three stages analogous to those usually observed in alloys subject to strain-induced MT [1]. For hydrogen-free crystals, a comparison of the values of start and finish temperatures for the forward and reverse MTs (M_s, M_f, A_s, A_f) determined from the $\rho(T)$ curve to the stages of $\sigma_{cr}(T)$ curves shows the following.

The first stage observed for 173 K < T < M_s is characterized by the normal temperature dependence of σ_{cr}, which is related to the thermoactivated motion of intervariant and twin boundaries of B19' martensite [1]. The minimum stresses σ_{cr} on the $\sigma_{cr}(T)$ curve are observed at $T = M_s$, which coincides with temperature M_s determined from the $\rho(T)$ curve. The maximum σ_{cr} values on the $\sigma_{cr}(T)$ curve correspond to temperature M_d at which the strain-induced MT start stress is equal to the plastic flow stress of the high-temperature B2 phase. The second stage, which corresponds to $M_s < T < M_d$, is characterized by an anomalous temperature dependence of σ_{cr}, which is related to the strain-induced nucleation of B19' martensite crystals [1]. The $\sigma_{cr}(T)$ curve at this stage is described by the Clapeyron–Clausius equation

$$\frac{d\sigma_{cr}}{dT} = -\frac{\Delta H}{\varepsilon_0 T_0}, \tag{1}$$

where ΔH is the change in the enthalpy upon the B2–B19' MT, ε_0 is the orientation-dependent lattice deformation, and T_0 is the temperature of chemical equilibrium of the B2 and B19' phases. At $T > M_d$, the $\sigma_{cr}(T)$ curve reveals the third stage, which is related to the plastic deformation of a high-temperature B2 phase.

Analysis of the data presented in Fig. 1 and the table leads to the following conclusions. First, hydrogen increases the M_s value as compared to that for the same alloy without hydrogen. Upon hydrogenation for 2 h, this value changes by $\Delta M_s = M_s^H - M_s(0) = 25$ K (where M_s^H and $M_s(0)$ are the MT start temperatures in hydrogenated and hydrogen-free crystals, respectively), while the hydrogenation for 4 h increases this value to $\Delta M_s = 48$ K in agreement with the data for TiNi polycrystals with similar compositions [3]. Second, hydrogenation leads to an increase in the critical stress at $T = M_s$ by $\Delta\sigma_{cr}(M_s) = \sigma_{cr}(M_s) - \sigma_{cr}^H(M_s)$ and for the high-temperature B2 phase $\Delta\sigma_{cr}^{B2}(400\text{ K}) = \sigma_{cr}^{B2(H)}(400\text{ K}) - \sigma_{cr}^{B2(H)}(400\text{ K})$ as compared to hydrogen-free crystals. Third, saturation with hydrogen leads to an increase in the value of $\alpha = d\sigma_{cr}/dT$.

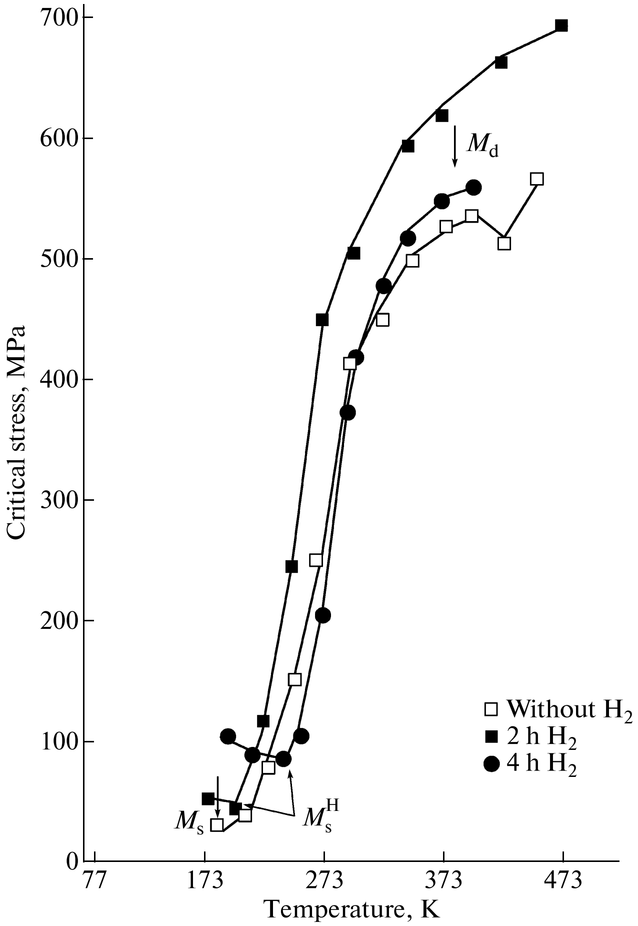

Fig. 1. Temperature dependences of critical axial stress σ_{cr} in tensile-tested single-phase $[\bar{1}11]$ single crystals of Ti–50.7% Ni (at %) alloy before and after hydrogenation.

Figure 2 presents results of investigation of the SME effect by cooling/heating at a tensile stresses 75 MPa in the interval of test temperatures from 77 to 400 K. Figure 3 shows the stress–strain (σ–ε) curve measured in tension upon 2-h hydrogenation. As can be seen from Fig. 2, both hydrogen-free and hydrogenated crystals at $\sigma = 75$ MPa are subject to single-stage B2–B19' MT that is fully reversible upon heating and exhibit the SME effect. The SME effect magnitude ε_{SME} in hydrogen-free crystals is 9% and close to theoretically calculated value of lattice deformation $\varepsilon_0 = 9.8\%$ for B2–B19' MT in a $[\bar{1}11]$-oriented crystal in tensiion [6]. Upon hydrogenation, the value of ε_{SME} at $\sigma = 75$ MPa is 2.5 times lower than in the initial crystal. These stresses are insufficient to cause fracture of the self-accommodating B19' martensite structure in hydrogenated crystals. Therefore, hydrogen increases the resistance to motion of the intervariant and twin boundaries in martensite as compared to that in the absence of hydrogen, which agrees with the increasing $\sigma_{cr}(M_s)$ value. Hence, in order to reach theoretical val-

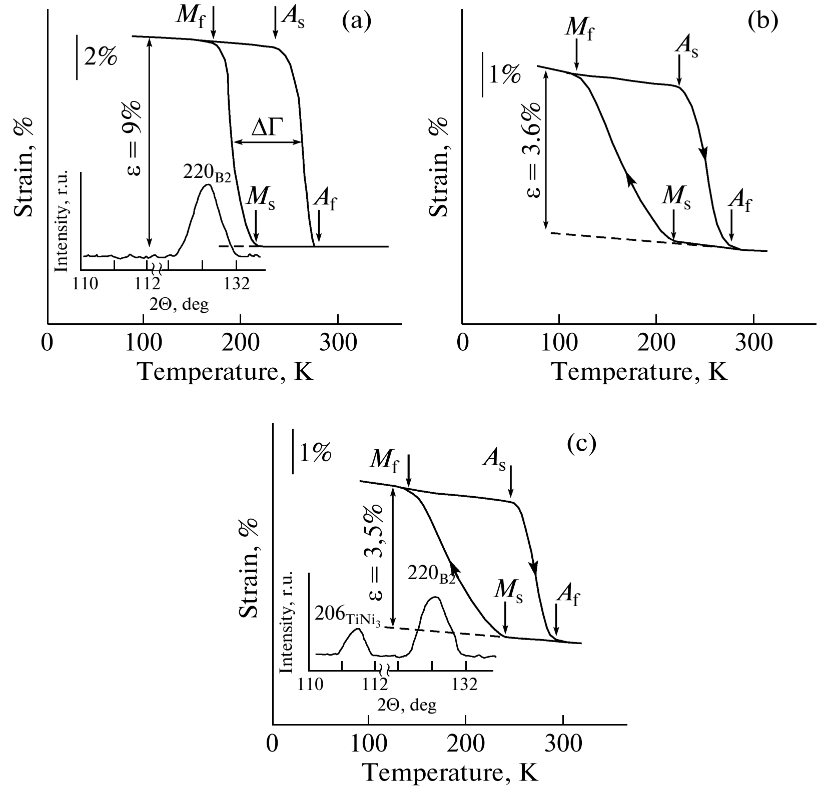

Fig. 2. SME magnitude at a constant tensile stress of $\sigma = 75$ MPa in $[\bar{1}11]$ single crystals of Ti–50.7% Ni (at %) alloy: (a) in the absence of hydrogen; (b, c) upon electrochemical hydrogenation at $T = 295$ K and current density $j = 1400$ A/m^2 for 2 and 4 h, respectively. The insets show the corresponding X-ray diffraction patterns of the phase composition of samples.

ues of lattice deformation ε_0 in hydrogenated crystals, it is necessary to increase external stresses.

In hydrogen-free $[\bar{1}11]$ single crystals, the SE in a temperature interval from A_f to M_d is not observed. At a preset strain of $\varepsilon_{exp} = 2.5\%$ in the first cycle, reversible deformation at $T = 274$ K is $\varepsilon_{rev} = 1\%$ and a perfect loop is not formed; at $\varepsilon_{exp} = 35\%$, the reversible deformation increases to 2.5%. The crystal is not fractured even at $\varepsilon_{exp} > 35\%$. Upon the 2-h hydrogenation, the SE on a level of 2.5% is observed at temperatures from 262 to 274 K and ε_{rev} amounts to 3% when $\varepsilon_{exp} = 12.5\%$ (Fig. 3). For $\varepsilon_{exp} > 12.5\%$, the hydrogenated crystals are subject to fracture. Upon 4-h hydrogenation, $\varepsilon_{rev} = 1\%$ and the samples are fractured even at $\varepsilon_{exp} > 4\%$.

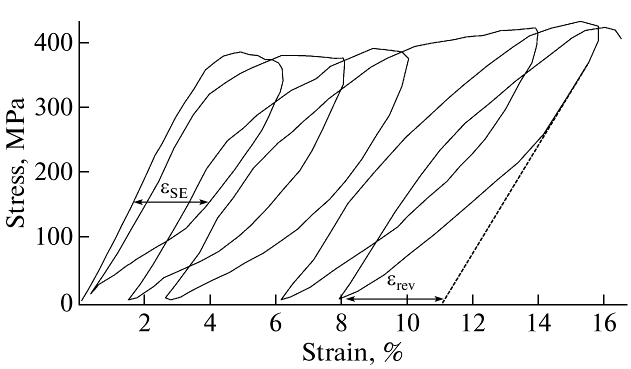

Fig. 3. Stress–strain (σ–ε) curve measured in tension at 262 K for a $[\bar{1}11]$ single crystal of Ti–50.7% Ni (at %) alloy upon 2-h electrochemical hydrogenation at $T = 295$ K and current density $j = 1400$ A/m^2.

The data in Fig. 2a show that, in hydrogen-free crystals, the values of supercooling $\Delta_1 = M_f–M_s$ and superheating $\Delta_2 = A_f–A_s$, as well as the magnitudes of thermal hysteresis $\Gamma_1 = A_f–M_s$ and $\Gamma_2 = M_f–A_s$, are equal to each other (see table) and, hence, the thermal hysteresis loop is symmetric. Hydrogenation leads to an increase in Δ_1, Δ_2, and Γ_2 values as compared to those for the hydrogen-free crystal (see table). As a result, the thermal hysteresis loop becomes asymmetric ($\Gamma_1 < \Gamma_2$). Previously, the asymmetric hysteresis loop was observed in crystals of Ti–51 at % Ni alloy at B2–R–B19' MT in precipitation of Ti_3Ni_4 particles [7]. As can be seen from Fig. 2 and the table, the reverse MT in the initial crystals starts at $A_s > M_s$, while the 4-h hydrogenation makes the A_s and M_s temperatures close to each other because hydrogen strongly affects M_s and weakly influences A_s [8].

The X-ray diffraction patterns of hydrogen-free crystals at room temperature showed the presence of diffraction peaks of the B2 phase, while the patterns of samples hydrogenated for 4 h contained the diffraction peaks of the B2 phase and $TiNi_3$ particles (see the inset to Fig. 2c). The measurements of thin crystalline foils hydrogenated for 4 h revealed titanium hydride (TiH) phase. Therefore, hydrogen possessing a high diffusion mobility at room temperature can favor the formation of a stable $TiNi_3$ phase, which usually appears in nonequiatomic TiNi alloys only as a result of long-term annealing at temperatures on the order of 850 K [1]. This conclusion agrees with data reported for hydrogenated single- and polycrystalline TiNi alloys [5, 8]. The formation of $TiNi_3$ and TiH phase particles in hydrogen-saturated TiNi crystals leads to a decrease in the Ni concentration in the matrix and the appearance of internal stresses due to a difference in the atomic parameters of these particles and the matrix. According to [9, 10] this causes an increase in M_s and a sharp decrease in the plasticity. The interaction of B19' martensite with $TiNi_3$ and TiH particles leads to an increase in $\sigma_{cr}(M_s)$ and Γ_2 for the reverse B19'–B2 MT and does not provide conditions for the SE [1]. In crystals hydrogenated for 2 h, the $TiNi_3$ and TiH phases were not detected by electron microscopy and X-ray diffraction techniques. Therefore, hydrogen upon 2 h saturation of samples occurs in the solid solution. This is confirmed by a significant increase in the level of internal stresses in the B2 phase, a small increase in $\sigma_{cr}(M_s)$, the appearance of SE and high plasticity in the martensite as compared to the crystals hydrogenated for 4 h.

Thus, the present investigation of $[\bar{1}11]$ single crystals of Ti–50.7% Ni (at %) alloy established that their electrochemical hydrogenation increases the M_s temperature and $\sigma_{cr}(M_s)$ axial stress level, decreases plasticity, and leads to the appearance of superelasticity. These phenomena are determined by induced phase changes in the hydrogenated TiNi alloy, including the formation of $TiNi_3$ and TiH particles.

Acknowledgments. This study was supported in part by the Ministry of Education and Science of the Russian Federation, project no. 16.1346.2014/K.

REFERENCES

1. K. Otsuka and C. M. Wayman, *Shape Memory Materials* (Cambridge University Press, Cambridge, 1998).
2. L. V. Spivak, Phys. Usp. **51** (9), 863 (2008).
3. I. A. Stepanov, Yu. M. Flomenblit, and V. A. Zaimovskii, Fiz. Met. Metalloved. **55** (3), 612 (1983).
4. M. Kh. Shorshorov, I. A. Stepanov, Yu. M. Flomenblit, and V. V. Travkin, Fiz. Met. Metalloved. **60** (2), 326 (1985).
5. B. L. Pelton, T. Slater, and A. R. Pelton, *Proceedings of SMST-97 Conference* (Asilomar Conference Center, Pacific Grove,1997), pp. 395–400.
6. H. Sehitoglu, R. Hamilton, D. Canadinc, X. Y. Zhang, K. Gall, I. Karaman, Y. Chumlyakov, and H. J. Maier, Metall. Mater. Trans. A **34** (1), 5 (2003).
7. E. Yu. Panchenko, Yu. I. Chumlyakov, I. V. Kireeva, A. V. Ovsyannikov, H. Sehitoglu, I. Karaman, and Y. H. J. Maier, Phys. Met. Metallogr. **106** (6), 577 (2008).
8. Yu. I. Chumlyakov, I. V. Kireeva, E. Yu. Panchenko, V. A. Kirillov, E. E. Timofeeva, I. V. Kretinina, Yu. N. Danil'son, I. Karaman, H. Maier, and E. Cesari, Russ. Phys. J. **54** (8), 937 (2012).
9. E. Hornbogen, V. Mertinger, and D. Wurzel, Scripta Mater. **44**, 171 (2001).
10. E. Hornbogen, Acta. Metall. **33** (4), 595 (1985).

Translated by P. Pozdeev